CHAPTER 5
ADAPTIVE LINEARIZATION OF THE MUSCLE PLANT

5.1. Fast Corrective Saccades vs. Slow Muscle Linearization

The use of outflow signals to determine present position at the HMI, and our outflow interpretation of the Shebilske (1977) data about corrective saccades (Section 4.11), do not deny that inflow signals play an important role in saccadic dynamics. In fact, our analysis stressed the need to linearize muscle plant responses to the outflow signals that determine present position at the HMI. In order to linearize muscle responses to outflow signals, information about the muscle plant's characteristics must somehow be used. Inflow signals supply this type of information. The process whereby inflow information is used is a slowly varying adaptive process. The corrective saccades studied by Shebilske (1977) occur on a much faster time scale than the adjustment of this slow recalibration process. Thus there is no contradiction in simultaneously advocating an outflow interpretation of the Shebilske (1977) data and an inflow interpretation of muscle linearization.

We will use the role of inflow in adaptive muscle linearization to explain several types of data, such as the data of Steinbach and Smith (1981) on the pointing behavior of patients after surgery on their extraocular muscles to correct strabismus (Section 5.4), and the data of Ron and Robinson (1973) and Vilis, Snow, and Hore (1983) concerning the role of the cerebellum in preventing dysmetria (Section 5.3).

5.2. Muscle Linearization Network

We hypothesize that a *Muscle Linearization Network* (MLN) exists wherein an inflow signal helps to linearize the size of a muscle contraction in response to outflow signals (Figure 5.1). This hypothesis does not imply that the muscle plant becomes more linear, but only that the muscle response to outflow signals becomes more linear, so that outflow signals can be used as a good estimator of present eye position in the HMI.

The MLN shares several basic design properties with the retinotopic command network (RCN) of Chapter 3. This comparison, as well as later ones in the text, will clarify our contention that distinct sensory-motor systems share common design features, including common brain regions. For example, in both the MLN and the RCN, the source of movement signals branches into two parallel pathways. One pathway generates an unconditioned movement signal. The other pathway generates a conditioned movement signal. This latter pathway passes through the AG stage, or cerebellum. The size, or gain, of the conditioned signal is determined by error signals to the AG stage. The unconditioned and conditioned movement signals then converge at a stage subsequent to the source of the unconditioned movement signal.

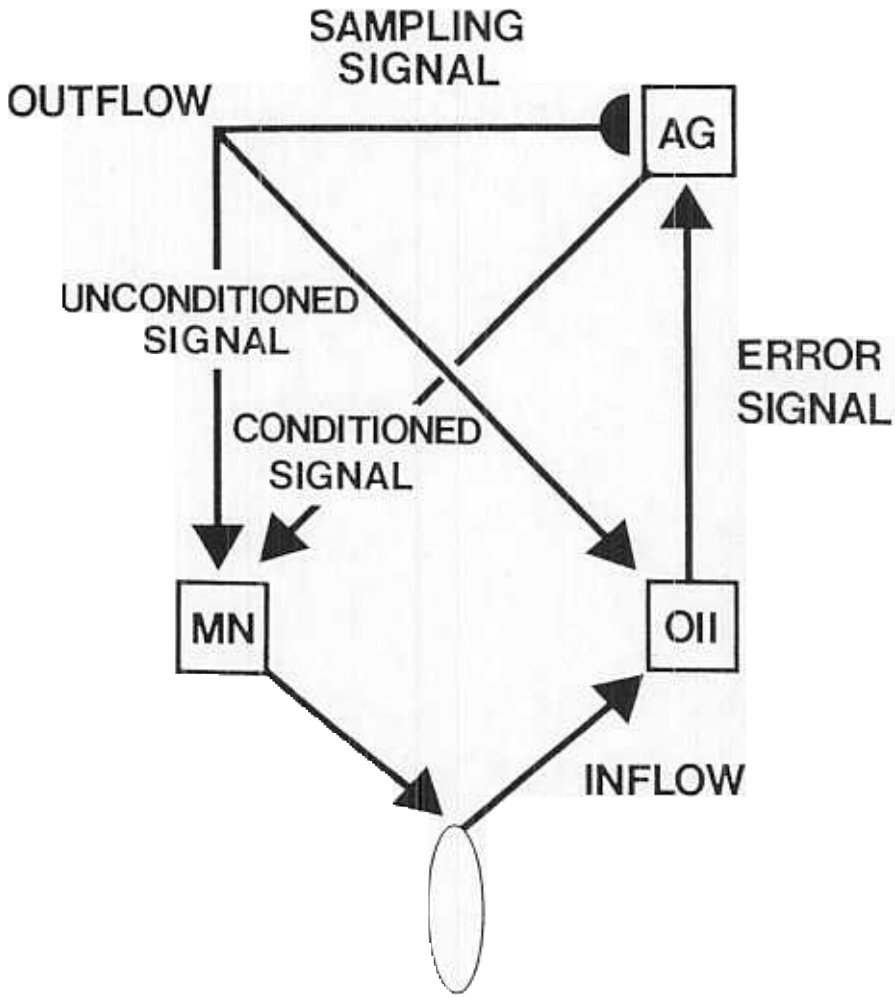

Figure 5.1. Some main features of the muscle linearization network, or MLN: The outflow-inflow interface (OII) registers matches and mismatches between outflow signals and inflow signals. Mismatches generate error signals to the adaptive gain (AG) stage. These error signals change the gain of the conditioned movement signal to the motoneurons (MN). Such an MLN adaptively linearizes the responses of a nonlinear muscle plant to outflow signals. The outflow signals can therefore also be used as a source of accurate corollary discharges of present eye position.

In the MLN, the unconditioned movement signal is clearly an outflow signal. The error signal is determined by a matching process that compares outflow signals with inflow signals, such that perfect matches generate no error signals and large mismatches generate large error signals. These error signals are delivered to the AG stage, where they alter the gain of the corresponding conditioned pathway. This conditioned pathway also arises from the source of outflow signals. The unconditioned and conditioned movement signals then converge at a stage subsequent to the source of outflow movement signals.

A number of informative technical problems must be solved in order for the MLN to work well. We will suggest solutions to these problems in stages. First, we will specify the MLN macrocircuit in greater detail. A possible macrocircuit is depicted in Figure 5.2. Fuchs and Becker (1981) noted the uncertainties of connectivity among brain stem saccade-related cells. The fact that modifications of the macrocircuit can achieve similar functional properties, and that modifications may exist across species, should be kept in mind throughout the subsequent discussion.

Figure 5.2 builds upon the conclusion (Keller, 1974, 1981; Luschei and Fuchs, 1972; Robinson, 1975) that medium lead burst (MLB) cells, which are the target cells of the saccade generator (SG), activate both tonic (T) cells and burst-tonic motoneurons (MN). The T cells, in turn, also excite the MN cells. The MN cells innervate the eye muscles which move and hold the eyes in place. The firing rate of T cells changes smoothly with eye position, whereas the firing rate of MN cells exhibits a burst during a saccade that returns to a position-dependent steady discharge level between saccades. Chapter 7 describes and models these cell types in greater detail.

We assume that the T cells are the source of the unconditioned outflow pathway to the MN cells. Given the other design constraints upon the MLN circuit, this hypothesis implies that the T cells also give rise to three other types of pathways. One pathway has already been mentioned: the pathway that provides corollary discharges to the HMI (Chapter 4). The other two pathways are used to control the conditioned movement signals that linearize the muscle response. One pathway sends excitatory signals to a network called the *outflow-inflow interface* (OII). The OII carries out the matching of outflow signals with inflow signals that generates error signals to the adaptive gain (AG) stage, or cerebellum. A non-zero error signal is generated only if a mismatch between outflow and inflow occurs. The fourth type of pathway from the T cells also reaches the cerebellum. This is the conditioned movement pathway that samples the error signals from the OII to the AG stage. This conditioned pathway thereupon projects to a stage subsequent to the T cells but prior to the muscles. We identify this target of conditioned movement signals as the MN cells.

In summary, the total saccade-related signal from the T cells to the MN cells is assumed to derive from a direct unconditioned pathway and an indirect conditioned pathway through the cerebellum. The size of the

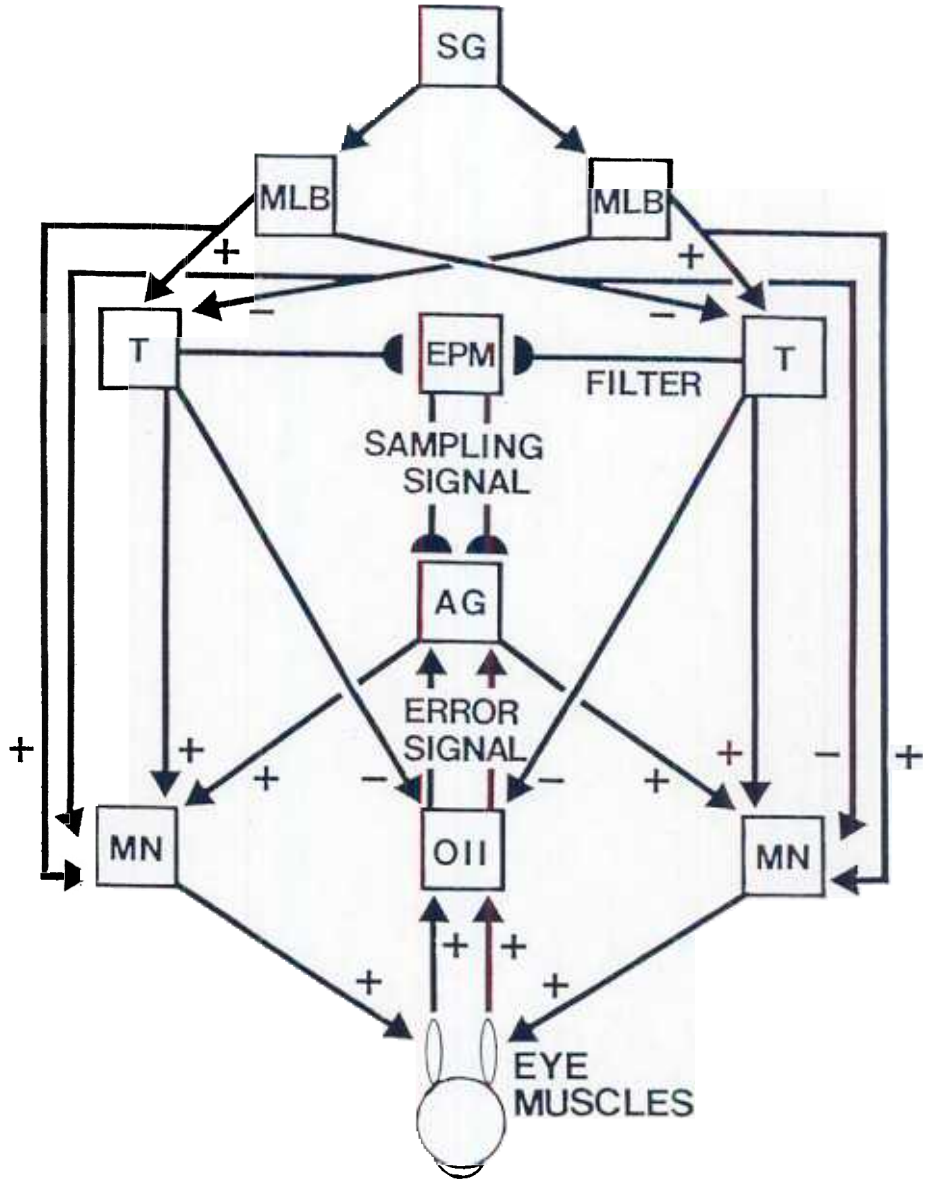

Figure 5.2. Some finer details of the muscle linearization network, or MLN: As in Figure 5.1, the OII generates error signals to the AG stage which alter the gain of the conditioned pathway to the MN. The sampling signals of these conditioned pathways are generated by an eye position map (EPM) which recodes outputs from tonic (T) cells of the saccade generator (SG). The medium lead bursters (MLB) of the SG excite their T cells and MN cells while they inhibit antagonist T cells and MN cells. The T cells also excite the corresponding MN cells and generate outflow signals to the OII, where they are matched against inflow signals.

conditioned signal is modified until a match between direct tonic cell outflow and muscle inflow is achieved. The conditioned pathway supplements the direct pathway signal until the muscle response to the direct pathway signal is linear. This property enables the output from the total tonic cell population to provide accurate corollary discharges to the HMI despite the existence of nonlinearities of muscle response in the absence of cerebellar compensation. It should be noted, however, that this sort of adaptive OII calibration does not guarantee accurate foveation. It merely guarantees a linear muscle response to whatever signals happen to activate the T cells.

5.3. Cerebellar Direct Response Cells

Before considering more technical questions about MLN design, we summarize two types of data that are clarified by the existence of a circuit like the MLN.

The existence of an indirect conditioned cerebellar pathway suggests an important role for oculomotor nuclei that occur between tonic cells and eye muscles. A cellular interface is needed at a stage subsequent to the tonic cells but prior to the muscles at which the total outflow signal, both unconditioned and conditioned, to the muscles can be computed. Figure 5.2 thus predicts the existence of a pathway from the AG stage, or cerebellum, to the MN cells of the oculomotor nuclei.

Ron and Robinson (1973) have reported the existence of saccade-related *direct response cells* in the dentate nucleus of the cerebellum. Direct electrical activation of these cells can elicit saccades with the remarkably short latency of 5–9 msec. These reaction times are consistent with the existence of a direct pathway from the direct response cells to the MN cells of the oculomotor nuclei. Our theory suggests that a subset of the direct response cells may be part of the conditioned movement pathway that linearizes muscle responses. If so, selective transection of this pathway should destroy the linearity of muscle responses.

Partial support for this hypothesis follows from the experiments of Vilis, Snow, and Hore (1983). These authors have shown that lesions of the medial cerebellar nuclei cause different degrees of dysmetria in different eye muscles. Such lesions do not, however, distinguish between cerebellar pathways to the oculomotor nuclei and to other saccade-controlling pathways, such as the SG. For example, in addition to direct response cells, Ron and Robinson (1973) have also reported the existence of cerebellar cells that elicit saccades with a much longer latency (12–16 msec.). These latter signals have properties compatible with their action at the SG. They may thus be part of the conditionable pathway of the RCN (Chapter 3). Hepp, Henn, Jaeger, and Waespe (1981) have described saccade-related burst-tonic mossy fibers in the cerebellar vermis having properties compatible with an SG action.

Thus, although many properties of these cerebellar pathways remain to be worked out, our theory provides a robust explanation of why certain cerebellar pathways should activate saccades at or before the SG, while

other cerebellar pathways should activate saccades at a much later processing stage, notably the MN cells. In fact, our theory suggests that a distinct cerebellar pathway, which helps to hold the eyes in a stable postural position between saccades, also projects to the MN cells (Chapter 8).

5.4. Adaptation to Strabismus Surgery

Steinbach and Smith (1981) have reported data that suggest a role for inflow signals in the eye movement control system. By contrast, the data of workers like Guthrie, Porter, and Sparks (1983) and Skavenski, Haddad, and Steinman (1972) have supported a role for outflow control and against inflow control. We now suggest how properties of the MLN can explain the Steinbach and Smith (1981) data without contradicting the data about outflow control.

Steinbach and Smith (1981) studied the arm-pointing behavior of patients who had been operated upon to correct strabismus. In such an operation, some eye muscles are detached from the eyeball and cut. Then the muscles are reattached to the eyeball to determine a new direction in which the eye will point at rest. After such an operation, a patient's eyes are bandaged for 7–48 hours. During this recovery period, a patient experiences no visual cues.

The arm-pointing behavior of patients was tested immediately after their bandages were removed. They were asked to point at test lights with one of their arms. The patients were not able to see their arms during this task. Despite the absence of visual signals of any kind, including visual error signals, during the bandaged interval, the arm-pointing behavior demonstrated a considerable amount of adaptation to the operation. The only obvious change due to the operation was in the eye muscles near their point of attachment, and not in the outflow pathways to them. These data thus suggest a role for inflow signals in controlling the adaptation process whereby conditioned outflow compensates for the operation.

This suggestion is further supported by Steinbach and Smith's observations of subjects who had experienced two successive strabismus operations. The Golgi tendon organs corresponding to the operated eye's medial rectus and lateral rectus muscles were thereby presumed to be destroyed. Adaptation to the eye's new position in its orbit was not observed in the pointing behavior of these patients. These data suggest that inflow signals, possibly mediated by the Golgi tendon organs, play an important role in this type of adaptation.

A possible explanation of these data in terms of MLN properties is the following. Suppose that a surgical lesion in an eye muscle alters the inflow signal that the muscle generates. Then mismatches between outflow signals and inflow signals can occur at the OII even when the patient's eyes are bandaged, since these outflow-inflow comparisons do not require visual signals. These mismatches generate error signals to the AG stage that slowly change the conditioned gain of the outflow signals. Two properties of this conditioned change cannot be explained until we more precisely

characterize the OII microcircuit; namely, why the adaptive change tends to compensate for the surgical lesion if the proprioceptors are spared, yet why no adaptation occurs if the proprioceptors are removed, even though such removal would seem to produce the biggest outflow-inflow mismatches. These issues thus probe finer aspects of how matches and mismatches are computed within the OII. For the moment, let us simply assume these properties of adaptation in order to complete our argument.

Even if we assume these properties, further argument is needed, because these properties do not in themselves explain how adaptation of an eye movement command can influence movement commands to the arms. To answer this question, we must ask how computations within the eye-head system generate movement commands to the hand-arm system. Our analysis of how circular reactions are learned (Section 1.3) suggests that such commands are mediated via head coordinate maps. In particular, the target position map, or TPM, of the eye-head movement system generates a command to the TPM of the hand-arm movement system.

This conclusion raises the possibility that the positional signals used to compute target positions in the TPM are inflow signals. The data of Guthrie, Porter, and Sparks (1983) seem to contradict this possibility, since vector compensation can occur normally in the absence of any inflow signals. If, however, outflow, rather than inflow, is used to compute target positions in the TPM, then how do changes in eye muscle inflow alter arm-pointing behavior at all?

We suggest that when the patient first sees the target light, no effect of the inflow change is experienced at the TPM. Instead, the subject's eyes saccade to foveate the target. This saccade benefits from the inflow-mediated changes in the total movement signal during the time that the eyes were bandaged. The saccade is therefore erroneous, but less erroneous than it would have been without the benefit of OII-driven gain changes. After this eye movement is over, the target light is again registered on the retina, at a new non-foveal position. This new retinal position can instate a new target position within the TPM. This second target position does reflect the inflow-mediated gain change. In fact, any further eye movements that the subject makes in an effort to foveate the target light can activate target positions at the TPM that reflect the inflow-mediated gain change. In the Steinbach and Smith (1981) experiment, subjects made from six to ten pointing responses. All but the first of these TPM target positions are suggested by the theory to activate pointing behavior which reflects adaptation to the surgical lesion.

One can test whether only this adaptive mechanism is recalibrated due to strabismus surgery by analysing pointing behavior that occurs before a patient moves his eyes. Then no major differences should exist between the arm-pointing behavior of patients who have had one strabismus operation and those who have had two strabismus operations.

Before describing OII design in greater detail, we pause to summarize some of the different concepts of "error correction" that have thus far arisen.

5.5. Error Correction with and without Adaptive Gain Changes

Data such as those of Steinbach and Smith (1981), Shebilske (1977), and Vilis, Snow, and Hore (1983) show that the term "error correction" must be used with care. Corrective saccades in the dark (Section 4.11) can use the HMI to "correct a saccadic error" without necessarily altering the parameters that control saccades. This is not the same type of "error correction" as occurs when second lights generate error signals that adaptively change the parameters of saccadic commands within the AG stage (Chapter 3). Indeed, in the Shebilske paradigm, there is no second light to act as an error signal, even though a corrective saccade can occur. Moreover, the HMI is part of the Vector Command Network, or VCN, whereas the second light error signals are elaborated as part of the Retinotopic Command Network, or RCN.

Conversely, a nonfoveating saccade can occur in which the light source is kept on and the outflow signal accurately encodes the vector command from the HMI. On such a trial, no corrective saccades of the Shebilske type will be generated if the target position and the final eye position agree at the HMI. However, adaptive learning could still occur because the second light is not foveated. Moreover, the nonfoveated second light can generate a second saccade. Such a second saccade, although tending to move the light towards the fovea, is not "corrective" in the Shebilske sense. Finally, inflow-mediated gain control of the outflow signal via the OII, albeit an adaptive change, is not the same adaptive change that causes accurate foveating saccades. The OII exists, moreover, in a different system: the Muscle Linearization Network, or MLN. One must clearly distinguish between VCN-mediated corrective saccades, RCN-mediated adaptive saccadic learning, RCN-mediated foveating second saccades, and MLN-mediated adaptive muscle compensation in order to avoid conceptual and terminological confusions.

5.6. Matching within the Outflow-Inflow Interface

The matching mechanism that we suggest for the OII helps to simultaneously solve several functional problems:

1. It can compensate for differences in the absolute size scales of outflow signals and inflow signals by computing the *relative* sizes of the signals corresponding to agonist-antagonist muscle pairs. Thus the computational unit within the OII is a spatial pattern, or normalized motor synergy (Section 1.10), rather than the amplitude of a single outflow or inflow signal.

2. It can match the inflow synergy against the outflow synergy. A perfect match occurs if the inflow synergy is a linear function of the outflow synergy. Poor matches occur if the inflow synergy exhibits nonlinear distortions. The error signal emitted from the OII increases as the match deteriorates.

3. Despite this last property, if the OII receives no inflow signals, then the muscle plant is not further linearized.

We will first summarize formal circuits that imply these properties before considering physical mechanisms that can generate their formal relationships. Several different, but closely related, formal circuits can achieve the desired properties. We summarize two of them to articulate the issues that need further neural data to be completely resolved. Two types of formal designs will be described, those in which the agonist inflow signal is an increasing linear function of the amount of agonist *contraction*, and those in which the agonist inflow signal is an increasing linear function of the agonist muscle *length*. Since amount of muscle contraction varies inversely with muscle length, these circuits embody testably different properties.

Figure 5.3 summarizes the main formal properties of an OII design whose inflow signals increase with muscle contraction. Figure 5.4 summarizes an OII model whose inflow signals increase with muscle length. Suppose that, within a prescribed time interval, the tonic cell outflow signal to an agonist muscle equals α and to the corresponding antagonist muscle equals β. Suppose that the muscle contractions caused by these outflow signals are $C(\alpha)$ and $C(\beta)$, respectively, and that the inflow signals are proportional to the amount of contraction; viz., $kC(\alpha)$ and $kC(\beta)$, where k is a positive constant.

The absolute sizes of these outflow signals and inflow signals might vary on very different size scales. We therefore assume that these size scales are normalized before their resultant spatial patterns are compared. Such a normalization scheme defines a "big" agonist outflow signal as one that is large relative to its antagonist contraction. Thus we assume that the outflow signal pattern (α, β) is transformed into the spatial pattern

$$\left(\frac{\alpha}{\alpha+\beta}, \frac{\beta}{\alpha+\beta}\right)$$

and that the inflow signal pattern

$$\big(kC(\alpha), kC(\beta)\big)$$

is transformed into the spatial pattern

$$\left(\frac{C(\alpha)}{C(\alpha)+C(\beta)}, \frac{C(\beta)}{C(\alpha)+C(\beta)}\right),$$

except if $k = 0$. If $k = 0$, equation (5.3) is replaced by $(0,0)$. Then the two spatial patterns are matched as follows.

The inflow spatial pattern (5.1) generates topographic excitatory signals and the outflow spatial pattern generates topographic inhibitory signals to the comparator region. Error signals are generated only if one of

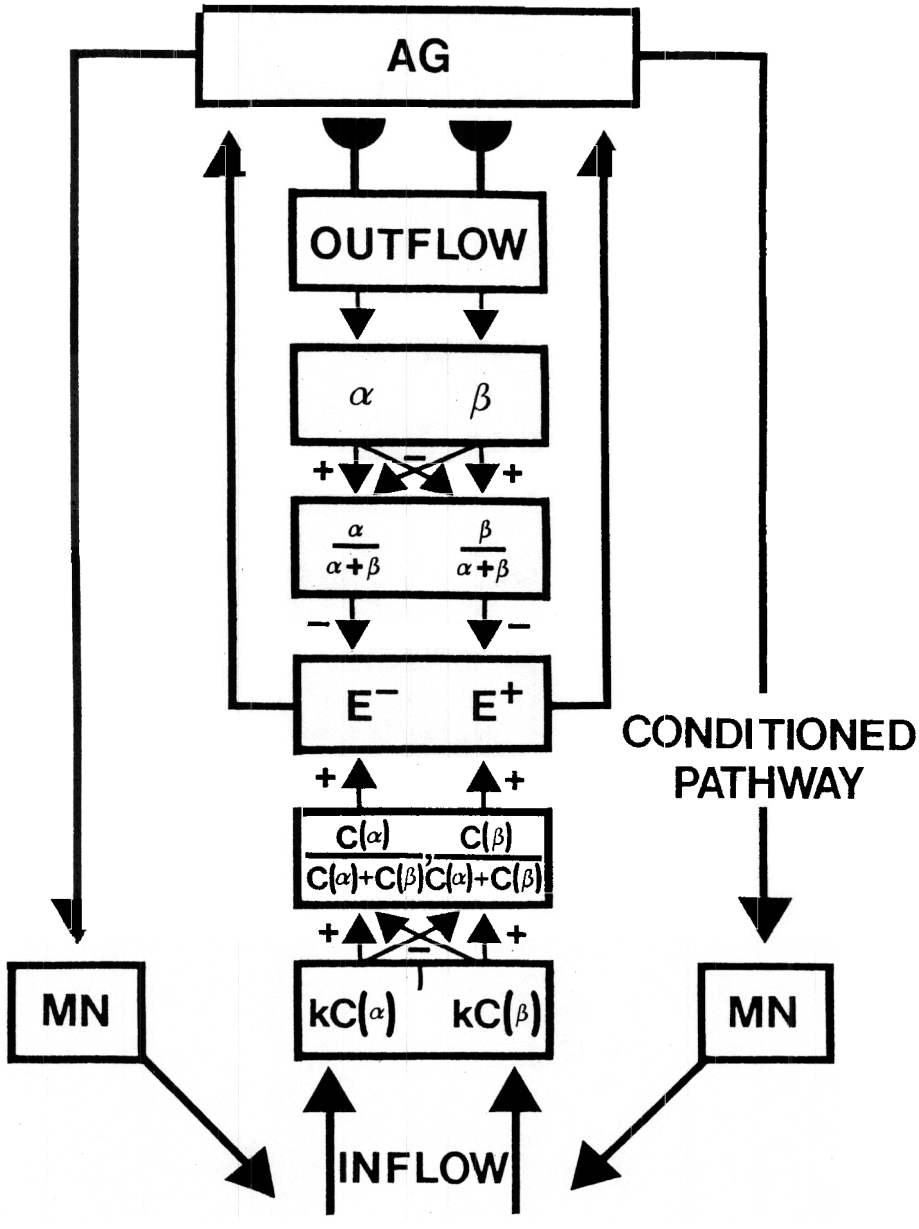

Figure 5.3. Microstructure of an outflow-inflow interface (OII) whose inflow signals vary monotonically with the amount of muscle contraction: See text for details.

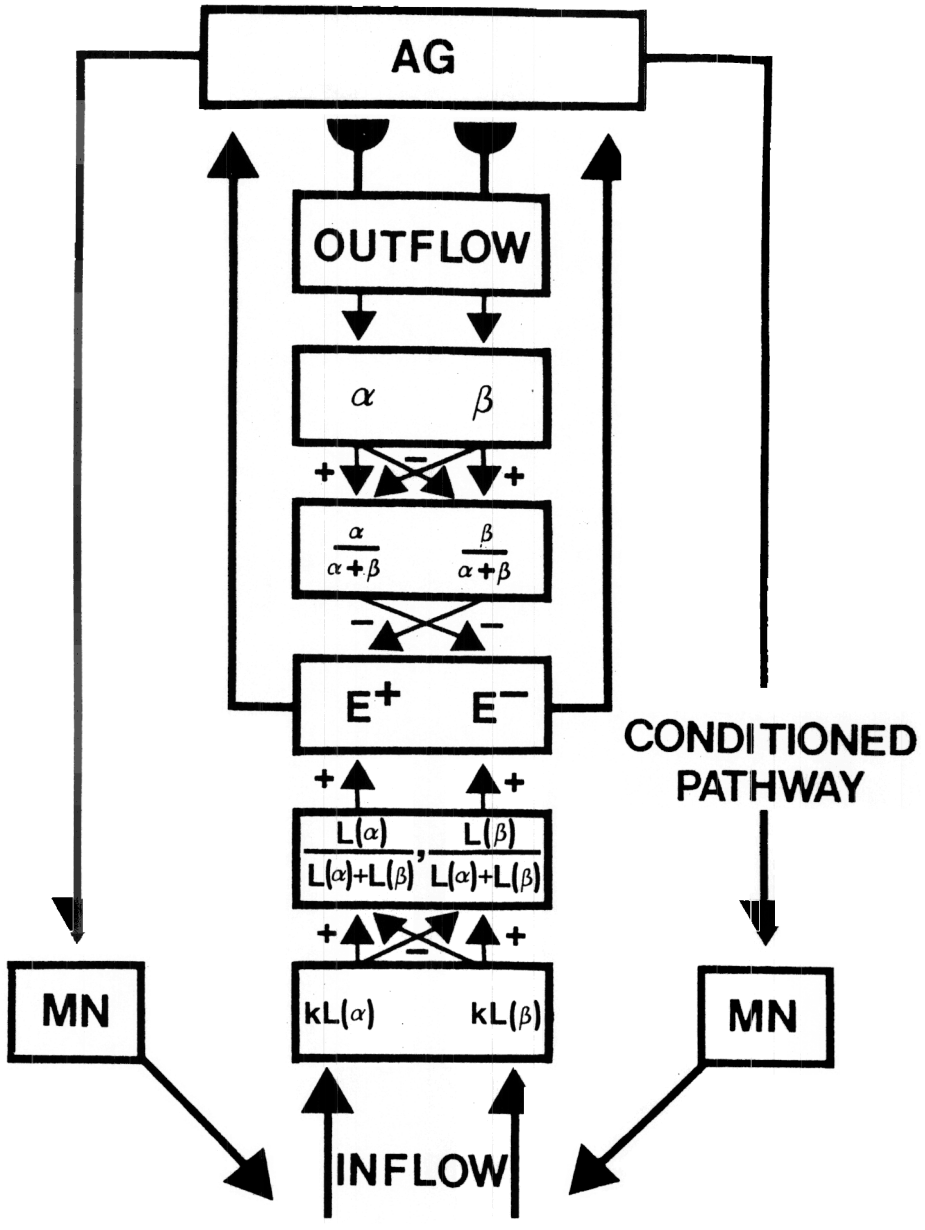

Figure 5.4. Microstructure of an outflow-inflow interface (OII) whose inflow signals vary monotonically with muscle length: See text for details.

the net potentials corresponding to the agonist inputs or antagonist inputs is positive. In other words, let

$$E^+ = \left[\frac{C(\beta)}{C(\alpha)+C(\beta)} - \frac{\beta}{\alpha+\beta}\right]^+$$

and

$$E^- = \left[\frac{C(\alpha)}{C(\alpha)+C(\beta)} - \frac{\alpha}{\alpha+\beta}\right]^+ \tag{5.5}$$

where $[\xi]^+ = \max(\xi, 0)$ and E^+ (E^-) is the agonist (antagonist) error signal. We suppose that the agonist error signal E^+ acts to increase the conditioned gain of the agonist muscle and to decrease the conditioned gain of the antagonist muscle within the AG stage. The antagonist error signal E^- has the opposite effect on these muscles at the AG stage. Thus the error signals generated by the OII and the error signals generated by second light error signals obey similar laws within the AG stage (Section 3.13).

To understand how these formal rules work, note that if the agonist muscle contracts less than its outflow signal command, then its conditioned gain is increased due to the OII-generated error signals in (5.4). Subsequent outflow signals therefore generate larger contractions and smaller error signals, until finally no error signals occur. To test whether no error signals occur when the muscle response is linearized, consider equations (5.4) and (5.5). Both error signals E^+ and E^- equal zero if

$$\frac{C(\alpha)}{C(\alpha)+C(\beta)} = \frac{\alpha}{\alpha+\beta}.$$

Equation (5.6) implies

$$\frac{C(\alpha)}{C(\beta)} = \frac{\alpha}{\beta}. \tag{5.7}$$

Thus error signals are not generated if the relative contraction and dilation of an agonist-antagonist muscle pair equals the relative size of the agonist-antagonist outflow signal. This is the basic linearity property that we seek. In particular, suppose that the agonist and antagonist outflow signals to the tonic cells mutually inhibit each other in a push-pull fashion, such that

$$\alpha + \beta = \gamma$$

where γ is constant. Also suppose that the amount of contraction of the agonist is balanced by the amount of dilation of the antagonist, such that

$$C(\alpha) + C(\beta) = \delta.$$

Then (5.7) implies

$$C(\alpha) = p\alpha,$$

where the proportionality constant $p = \gamma^{-1}\delta$.

Suppose, by contrast, that the agonist muscle contracts nonlinearly in response to the outflow signals; for example, suppose that the agonist muscle contracts too little. Then by (5.4) and (5.5),

$$E^+ > 0 = E^-, \tag{5.11}$$

so that the agonist conditioned gain will be increased and the antagonist conditioned gain will be decreased due to conditioning. The inequalities (5.11) are due to the fact that the match of *agonist* signals in (5.5) gives rise to the *antagonist* error signal, and the match of *antagonist* signals in (5.4) gives rise to the *agonist* error signal. This model predicts that the agonist-antagonist symmetry axis is reversed somewhere between the OII, which is a target for the outflow and inflow signals from the tonic cells and muscles, respectively, and the cerebellum, which receives OII-activated error signals via climbing fibers. The model of Figure 5.4, in which length-based inflow signals are used, also predicts a reversal of symmetry axis. This reversal occurs, however, within the OII in the matching of outflow and inflow signals.

5.7. An Explanation of the Steinbach and Smith Data

Equations (5.1)–(5.5) provide an explanation of why an absence of inflow signals prevents adaptation to strabismus surgery. If all inflow signals are prevented, then, since the inflow constant $k = 0$ in equation (5.2), equations (5.4) and (5.5) reduce to

$$E^+ = [-\frac{\beta}{\alpha+\beta}]^+ = 0 \tag{5.12}$$

and

$$E^- = [-\frac{\alpha}{\alpha+\beta}]^+ = 0, \tag{5.13}$$

so that no error signals at the AG stage are generated. Another way to state this conclusion is in terms of inflow signals to the cerebellum. In equations (5.4) and (5.5), inflow signals provide the excitatory drive for generating error signals to the cerebellum. This model predicts that cutting all inflow pathways will eliminate a major source of inflow which reaches the cerebellum via climbing fibers. Cutting all of these inflow pathways should also prevent the eye movement system from linearizing muscle responses after nonlinearities are induced by other experimental manipulations. Cutting the inflow pathways need not disrupt the linearity of muscle response in the absence of other experimental manipulations, because the inflow signals give rise to error signals, not to the conditioned movement signals that maintain a linear muscle response.

We can now show how the effects of strabismus surgery are compensated for by this OII model. Suppose that an agonist muscle is cut and

shortened before being reattached to the eyeball. Suppose that such an operation has two simultaneous effects: It causes the eye to point more in the direction of the agonist muscle, and it weakens the inflow signal from this muscle. Due to the weakening of the agonist inflow signal, equations (5.4) and (5.5) imply that

$$E^+ = 0 < E^-. \tag{5.14}$$

Consequently, the gain of the antagonist muscle will increase, thereby tending to shift the eye back towards its original position. One might therefore ask why strabismus surgery does not always fail? The theory suggests two reasons: The backward shift merely tends to relinearize the muscle responses. Second light error signals assume the major load of recalibrating the conditioned gains which will ensure accurate foveation despite the surgical change in eye position.

5.8. A Role for Golgi Tendon Organs in Muscle Linearization

Steinbach and Smith (1981, p.1408) concluded from their data "that in some not yet understood way the tendon end organs are important elements in a scheme for eye position proprioception...This is a difficult hypothesis because all established facts about tendon organ function indicate a role in phasic responses to stretch and never any suggestion of a role in supplying positional information." The models in Figure 5.3 and 5.4 indicate two different ways in which Golgi tendon organs might contribute to muscle linearization. Both of these models are based upon observations that Golgi tendon organs respond to increases in muscle tension. Tendon organs exhibit a high threshold when activated by passive stretch, but are exquisitely sensitive to active muscle contraction (Granit, 1962; Houck and Henneman, 1967; Kandel and Schwartz, 1981). Thus during active contraction of an agonist eye muscle, its Golgi tendon organs can emit an output signal that increases with the amount of muscle contraction. Since the antagonist muscle is passively stretched during an active agonist contraction, its Golgi tendon organ may respond much less, or not at all. If the antagonist tendon organ does respond, however, its signal would be expected to increase, rather than decrease, due to the progressive contraction of the agonist muscle. Data concerning the properties of Golgi tendon organs during saccadic eye movements seem not to be available, so our discussion of this matter will consider several mechanistic possibilities that are compatible with functional requirements.

One possibility is that, as an agonist muscle contracts, the increase of MN input to the agonist muscle coexists with a progressive decrease in MN input to the antagonist muscle. Such a decrease could cause a progressive reduction of tension in the antagonist muscle. The increase in $C(\alpha)$ and the decrease in $C(\beta)$ that was assumed in equation (5.3) could hereby be achieved. Van Gisbergen, Robinson, and Gielen (1981), by contrast, have shown that the MN input to the antagonist muscles of monkeys are totally shut off during saccades. Thus a different source of progressively

decreasing antagonist inputs $C(\beta)$ is needed to establish the ratio scale in equation (5.3).

One possibility is that the Golgi tendon organs of the agonist muscle provide the input for both $C(\alpha)$ and $C(\beta)$ using a push-pull mechanism. Figure 5.5 depicts such a mechanism. Figure 5.5 is based upon the hypothesis that there exist agonist and antagonist tonic cell populations which receive push-pull inflow inputs from the contracting muscle. These tonic cells, in turn, input to the mechanism that computes the ratio scale. Thus, suppose that during an agonist contraction, the agonist inflow signal is $kC(\alpha)$ and the antagonist inflow signals is approximately 0. Let the baseline activity of both the agonist and the antagonist tonic cell populations equal M. Then their activities after inflow input are

$$\big(M + kC(\alpha), M - kC(\alpha)\big). \tag{5.15}$$

Since M is larger than the maximal inflow signal, both terms in (5.15) are nonnegative. Next, the activities (5.15) generate a spatial pattern

$$\Big(\frac{1}{2}\big(1 + \frac{kC(\alpha)}{M}\big), \frac{1}{2}\big(1 - \frac{kC(\alpha)}{M}\big)\Big). \tag{5.16}$$

Each activity in (5.16) is computed by dividing the corresponding activity in (5.15) by the sum of both activities in (5.15). Equation (5.16) is now used instead of (5.3) to compute the error signals E^+ and E^- in (5.4) and (5.5). Thus

$$E^+ = \Big[\frac{1}{2}\big(1 - \frac{kC(\alpha)}{M}\big) - \frac{\beta}{\alpha + \beta}\Big]^+ \tag{5.17}$$

and

$$E^- = \Big[\frac{1}{2}\big(1 + \frac{kC(\alpha)}{M}\big) - \frac{\alpha}{\alpha + \beta}\Big]^+. \tag{5.18}$$

To test whether no error signal is emitted when the muscle response is linearized, we set E^+ and E^- equal to zero, as in Section 5.6. No error signal is emitted if

$$C(\alpha) = \frac{M}{k}\Big(\frac{\alpha - \beta}{\alpha + \beta}\Big). \tag{5.19}$$

If, moreover, agonist and antagonist outflow signals to the tonic cells are mutually inhibitory, as in (5.8), then

$$C(\alpha) = q\alpha - r \tag{5.20}$$

where $q = 2M(k\gamma)^{-1}$ and $r = M(k)^{-1}$. Thus this model also generates error signals until the amount of muscle contraction is a linear function of the outflow signals. All of our other conclusions about muscle linearization and about the Steinbach and Smith (1981) data also hold, with the

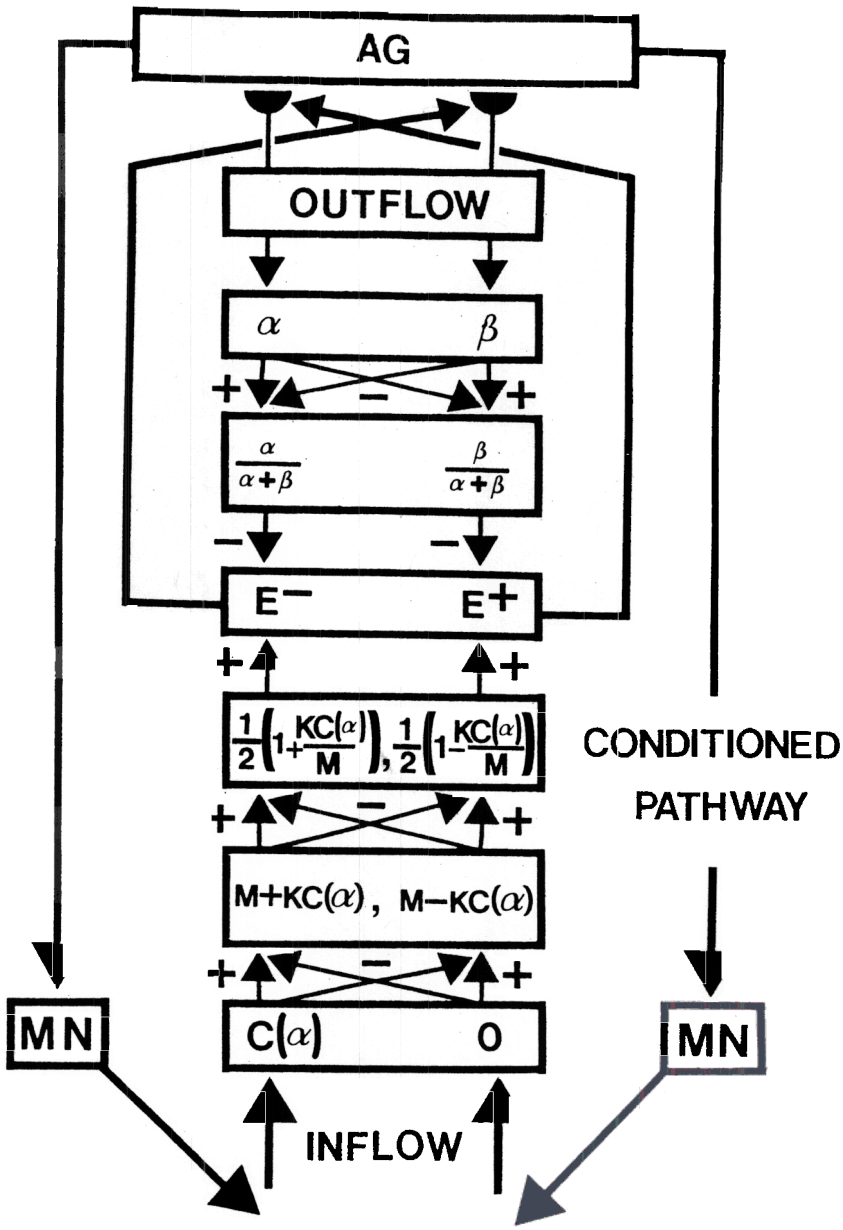

Figure 5.5. Microstructure of an outflow-inflow interface (OII) whose inflow signals are derived only from the muscles that are actively contracting: See text for details.

exception of one refinement. If all inflow signals are cut in Figure 5.5, then the tonic cells continue to register basal activities (M, M), and the normalized pattern $(\frac{1}{2}, \frac{1}{2})$ continues to input to (E^-, E^+). Thus error signals $E^+ = [\frac{1}{2} - \frac{\beta}{\alpha+\beta}]^+$ and $E^- = [\frac{1}{2} - \frac{\alpha}{\alpha+\beta}]^+$ can reach the AG stage. These error signals will not influence muscle linearization, however, if there are approximately as many eye movements in an agonist direction as there are in the corresponding antagonist direction, because both error signals are measured relative to the value $\frac{1}{2}$.

For completeness, we note that an alternative model, based upon length-dependent inflow signals (Figure 5.4), is also consistent with the Steinbach and Smith (1981) data. The length-dependent inflow signals would be derived from the muscle spindles (Granit, 1962; Kandel and Schwartz, 1981), rather than from the Golgi tendon organs. A single strabismus operation could alter the match between inflow length information and outflow commands. It remains to say how destruction of all inflow signals from the Golgi tendon organs could prevent adaptation. In a spindle-based model, these data seem to require the assumption that inflow from the Golgi tendon organs is also used. Such inflow would not, however, be used to compute the state of muscle contraction. It would act to nonspecifically gate the error signals to the cerebellum. Only during active muscle contractions would these error gates be activated, thereby enabling muscle linearization to occur.

5.9. Dynamic Linearization: Adaptive Sampling during Saccades

All of the above models of the OII share an important, and surprising, functional property. They all predict that the cerebellar learning which linearizes eye muscle responses takes place *during* saccades, and at a very fast sampling rate. In models which use Golgi tendon organ inflow, as in equation (5.15), this conclusion follows from the fact that, during posture, agonist and antagonist tensions must be equal in order to hold the eye in a fixed position. Hence, after a saccade is over, the outputs from both agonist and antagonist Golgi tendon organs should be equal too. Their ratio cannot, therefore, be used to compute deviations from muscle linearity. In a spindle-based model, as in Figure 5.4, the Golgi tendon organ output that gates cerebellar error signals would be expected to be much larger during a saccade, when the agonist muscle is actively contracting, than after. Hence error signals would be much more effective during a saccade in this model too.

The idea that adaptive sampling takes place during a saccade makes sense from an intuitive vantage point. The forces on the eye muscles during a saccade are very different from the forces that act between saccades. Hence conditioned gains that were learned during posture might be the wrong gains to ensure muscle linearity during movement. Furthermore, if one waits until a movement is over to learn these gains, then the accumulated nonlinearity due to an entire saccade would have to be compensated

for at the terminal saccadic position. By contrast, if the learning circuit is fast enough to deliver sampling and error signals several times during a saccade, say within 15 or 20 msec., then conditioned gains could be learned for components of each saccadic movement in which not too much nonlinearity has accumulated. The saccade would hereby be broken down into movement "frames," each of whose nonlinear distortions could separately be dealt with as a function of eye position within that frame.

If the model is confirmed in which Golgi tendon organs supply inflow to the OII, it will provide a new functional role for these organs as sensors of dynamic muscle contraction, as well as for the rapid conduction velocity of their afferent fibers.

Two more mechanisms need to be specified to complete our discussion of OII design.

5.10. An Agonist-Antagonist Ratio Scale

This section suggests a simple mechanism whereby an input pattern (I_1, I_2) can be transformed into a spatial pattern

$$\left(\frac{I_1}{I_1 + I_2}, \frac{I_2}{I_1 + I_2}\right). \tag{5.21}$$

The transformations (5.1), (5.3), and (5.16) within the OII are all special cases of this problem. The desired transformation can be accomplished by a feedforward on-center off-surround network whose cells obey membrane equations (Section 2.6). In the special case of an agonist-antagonist interaction, an on-center off-surround anatomy is a push-pull anatomy.

Let $x_1(t)$ be the potential of the agonist population and $x_2(t)$ be the potential of the antagonist population. A simple version of the networks used in Section 2.6 is sufficient. Suppose that

$$\frac{d}{dt}x_1 = -Ax_1 + (B - x_1)I_1 - x_1 I_2 \tag{5.22}$$

and

$$\frac{d}{dt}x_2 = -Ax_2 + (B - x_2)I_2 - x_2 I_1. \tag{5.23}$$

Define the total input $I = I_1 + I_2$. Then (5.22) and (5.23) can be rewritten as

$$\frac{d}{dt}x_1 = -Ax_1 + BI_1 - x_1 I \tag{5.24}$$

and

$$\frac{d}{dt}x_2 = -Ax_2 + BI_2 - x_2 I. \tag{5.25}$$

If the potentials x_1 and x_2 equilibrate quickly to changes in the inputs I_1 and I_2, then $\frac{d}{dt}x_1 \cong 0$ and $\frac{d}{dt}x_2 \cong 0$ at all times. Thus

$$x_1 \cong \frac{BI_1}{A + I} \tag{5.26}$$

$$x_2 \cong \frac{BI_2}{A + I}. \tag{5.27}$$

If the total input I exceeds constant A by a sufficient amount, then

$$x_1 \cong \frac{BI_1}{I_1 + I_2} \tag{5.28}$$

and

$$x_2 \cong \frac{BI_2}{I_1 + I_2}. \tag{5.29}$$

The desired transformation can thus be defined by

$$(I_1, I_2) \rightarrow (x_1, x_2). \tag{5.30}$$

5.11. Sampling from a Spatial Map of Outflow Position

We assume that the tonic (T) cells in Figure 5.2 are the source of outflow signals to the MN cells as well as the source of sampling signals to the AG stage. The T cells cannot, however, project directly to the AG stage, for the same reason that the HMI cannot project directly to the AG stage. Sufficiently different spatial patterns of activity must give rise to different sampling pathways with their own LTM traces. Only in this way can different outflow patterns learn different conditioned gains to compensate for different degrees of muscle nonlinearity at different eye muscle positions.

The T cell and HMI examples hereby focus our attention upon a functional problem that is of general importance: How can activity patterns across a fixed set of cells be parsed by a spatial map, such that sufficiently different patterns activate different cell populations within the spatial map? The next chapter addresses this issue.

Within the MLN, sufficiently distinct tonic cell outflow patterns activate different cellular locations within such a spatial map. We therefore call the map an *eye position* map (EPM). Each spatial locus in the EPM sends a separate sampling pathway to the cerebellum. Each such pathway adaptively encodes all gain changes that are caused by OII-induced error signals while the sampling pathway is active. These gain changes, in turn, differentially alter the cerebellar feedback signals to the MN cells of the oculomotor nuclei. Chapter 3 explains how a single sampling pathway can simultaneously encode gain changes that differentially influence all the eye muscles and thereby control all the eye muscles in a synergetic, or coarticulated, fashion.